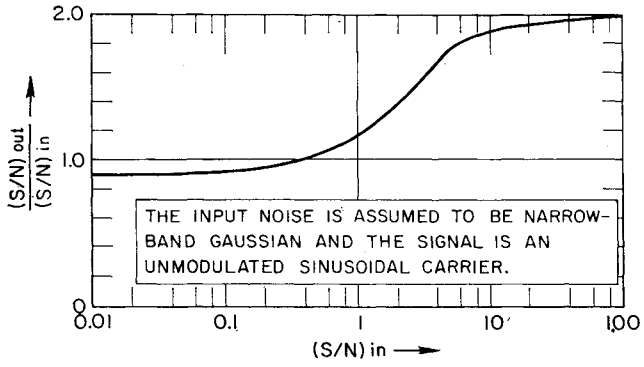

Fig. 8 Baghdady's result for a bandpass limiter whose output and input noise bandwidths are equal.

the results obtained by Baghdady[5] (Fig. 8). Thus, $N_t = \gamma_n N_s$, and

$$\sum_j I_{tj} = \sum_j \gamma_j I_{sj}$$

Substituting these into Eq. (9) and normalizing to S_s yields

$$\frac{S_0}{N_0} = \left(\frac{C}{N}\right)_L \left[1 + \gamma_n \frac{N_s}{S_s} + \frac{1}{S_s}\Sigma\gamma_j I_{sj} + \left(\frac{C}{N}\right)_L \left(\alpha\gamma_n \frac{N_s}{S_s} + \frac{1}{S_s}\sum_j \beta_j\gamma_j I_{sj}\right)\right]^{-1} \quad (10)$$

which is the basic expression for link behavior. The first three terms within the brackets represent power division, and the last two represent the degradation due to interference and noise. Note that S_0/N_0 is a predetection ratio. If the detector has a processing gain G_p, then the postdetection ratio is $(S/N)_D = (S/N)_0 G_p$. In the case of a correlation detector, G_p is simply the ratio of pre- and postdetection bandwidths; $(S/N)_D$ may also, of course, represent a required detection threshold.

The following three cases can be deduced from Eq. (10):

1) *n equal noiselike, pseudo-random signals, with their spectra completely overlapping, and with all bandwidths (signal, receiver, and satellite) equal:* Thus, all $\beta_j = 1$, and the I_{sj}'s are $(n-1)$ of the equal signals, so that

$$\frac{S_0}{N_0} = \left(\frac{C}{N}\right)_L \left[1 + \gamma\left(\frac{N_s}{S_s} + n - 1\right) + \left(\frac{C}{N}\right)_L \times \left(\frac{N_s}{S_s} + n - 1\right)\gamma\right]^{-1} \quad (11)$$

Figure 6 was plotted from this equation using both CCIR standards and reduced "adequate" voice standards. Notice that n appears twice, since the signals not only divide power but look like additional noise to each other.

2) *One signal, with jamming greatly in excess of the satellite noise:* Then N_s is assumed negligible, and $\beta_1 = \beta$, $\beta_2 = \beta_3 = \ldots = \beta_j = 0$, and $\sum_j \gamma_j I_{sj} = \gamma J$. Substituting these relations into Eq. (10) and assuming that the satellite, signal, and receiver have identical bandpasses, we have

$$\frac{S_0}{N_0} = \left(\frac{C}{N}\right)_L \left[1 + \gamma\frac{J}{S_s} + \left(\frac{C}{N}\right)_L \beta\gamma\frac{J}{S_s}\right]^{-1} \quad (12)$$

This equation was used to plot Fig. 7, assuming $\beta = 1$.

3) *The commercial FDM case, with n equal but nonoverlapping signals:* $\sum_j \gamma_j I_{sj} = (n-1)S_s\Sigma\gamma_j$. If the n input signals are equal, they will stay so, and the γ_j may be put equal to unity; in addition, all $\beta_j = 0$, so that

$$\frac{S_0}{N_0} = \left(\frac{C}{N}\right)_L \left[n + \gamma\frac{N_s}{S_s} + \left(\frac{C}{N}\right)_L \alpha\gamma\frac{N_s}{S_s}\right]^{-1} \quad (13)$$

In this case, calculation of S_0/N_0 must include the effects of companding, FM improvement factor, the use of voice statistics, and intermodulation noise, so that Eq. (13) is virtually impossible to use as it stands. It is worth noting that n appears only once for power division, since the signals are not selfinterfering. Thus, it does illustrate the difference between "vertically" and "horizontally" stacked modulated channels.

References

[1] Pritchard, W. L. and MacGregor, N., "Military vs commercial Comsat design," Astronaut. Aeronaut. **2**, 70 (October 1964).

[2] Fagot, J. and Magne, P., *Frequency Modulation Theory* (Pergamon Press, London, 1961).

[3] "Recommendations," *CCIR Documents of the 9th Plenary Assembly, Los Angeles,* **1959** (International Telecommunications Union, Geneva, Switzerland, 1959), Vol. 1, Sec. F.

[4] "A system of multiple access for satellite communications," Bell Telephone Labs., Communication Satellite Corp. Contract CSC-CD-101.

[5] Baghdady, E. J. (ed.), *Lectures on Communication System Theory* (McGraw-Hill Book Co., Inc., New York, 1961), p. 540.

Refrigeration in Space by the Fluidized Technique

FRANK J. HENDEL* AND J. C. MULLIGAN†
North American Aviation, Inc., Downey, Calif.

Nomenclature

A	=	inside tube area, ft²
C	=	suspension concentration, lb carbon/lb suspension
c_p	=	specific-heat capacity, Btu/lb-°R
D	=	inside tube diameter, in.
G	=	suspension flow rate, lb/hr
h	=	heat-transfer coefficient of suspension, Btu/hr-°R-ft²
k	=	thermal conductivity, Btu/hr-°R-ft²/in.
$K, m, n,$	=	const
P	=	suspension pressure, lb/ft²
R	=	gas constant, 386 ft/°R for He
T	=	absolute temperature, °R
V	=	suspension velocity, fps
Nu, Re, Pr	=	Nusselt, Reynolds, and Prandtl numbers, respectively
ϵ	=	suspension voidage, ft³ He/ft³ suspension
μ	=	absolute viscosity, lb/ft-sec
ρ	=	density, lb/ft³

Subscripts

C	=	carbon
He	=	gaseous helium
s	=	suspension (carbon in He)

CRYOGENIC fluids will be needed in future space operations as propellants, for life support, for electrical power generation, pressurization of propellant tanks, pneumatic controls, and cooling.

Received August 14, 1964; revision received March 1, 1965.

* Staff Scientist; now Engineering Specialist, Jet Propulsion Laboratory, California Institute of Technology, Pasadena, Calif.; also Instructor of courses on Space Vehicles and Missiles at the University of California at Los Angeles, Los Angeles, Calif. Associate Fellow Member AIAA.

† Research Engineer; now at University of Mississippi, Chemical Engineering Department.

During space operations of long duration it will be necessary to store cryogenic fluids with minimum losses. A fluidized technique for cooling of cryogenic fluids has been proposed by the first author.[1] Minute particles of graphite (or another suitable solid) are held in suspension by gaseous helium, which circulates rapidly in the refrigeration system (Fig. 1). The cold suspension passes through coils within the cryogenic storage tank to remove heat from the stored fluid; it then passes into a space radiator, which can be provided with flexible connections, if necessary, to enable proper orientation of the radiator. The refrigerating suspension is best circulated by a positive rotary-type blower, as illustrated. The presence of graphite (carbon) particles enhances the heat-transfer processes within the cooling coils and the space radiator. This enhancement is caused primarily by the high thermal conductivity of carbon. A further increase is achieved by keeping the suspension under a high pressure. The area of the space radiator and of the coil will vary inversely with carbon concentration, whereas the energy required to circulate the suspension will vary directly with carbon concentration.

Thermal properties of the suspension, together with suitable mathematical expressions, are necessary to calculate the probable heat transfer in the fluidized refrigeration system. Properties of helium have been taken at a pressure of 1 atm. Since no data were available for thermal conductivity of graphite (preferred because of its lubrication properties) at cryogenic temperatures, data for natural carbon were used. The following equations (weighted sum technique) were used to estimate the thermal conductivity and heat capacity of the suspension as functions of carbon concentration (lower part of Fig. 2) at various temperatures:

$$k_s = Ck_C + (1 - C)k_{He} \quad (1)$$

$$c_{ps} = Cc_{pC} + (1 - C)c_{pHe} \quad (2)$$

Wall-to-Fluid Heat Transfer

In addition to increasing the thermal conductivity, the minute solid particles in the heat-transfer fluid tend to induce turbulence in the fluid film on the tube wall and thus increase heat transfer. Although progress is being made in the analysis of heat transfer in turbulent flow, most of the calculations are made with semiempirical equations based on correlations of experimental data. The most widely accepted relationship describing turbulent, convective heat transfer in single-phase fluids is

$$Nu = KRe^m Pr^n \quad (3)$$

Efforts to improve the correlation of data usually have resulted in only slightly differing values for the constants K, m, and n, the most widely used values being 0.023, 0.8, and 0.4, respectively.[3] With a slightly different value for K, Eq. (3) has been applied to heat transfer from suspensions of silica-alumina gel in air.[2] Written explicity for h and in terms of flow rate, this equation takes the form

$$h = 0.025 \frac{k_s}{D} \left(\frac{D\,G}{43{,}200\,\mu_s A} \right)^{0.8} \left(\frac{43{,}200\,c_{ps}/\mu_s}{k_s} \right)^{0.4} \quad (4)$$

where all of the suspension properties are evaluated at suspension temperature.

Other equations that are applicable in determining the variation in suspension viscosity with variations in temperature and concentration of solids are[3]

$$\mu_s = \mu_{He} \exp[4.1(1 - \epsilon)/(0.64 - \epsilon)] \quad (5)$$

where

$$\epsilon = 1 - C\rho_s/\rho_C \quad (6)$$

and

$$\rho_s = \rho_C\rho_{He}/[\rho_C - C(\rho_C - \rho_{He})] \quad (7)$$

An average value of 135 lb/ft³ can be assumed for the density of solid carbon. The density of gaseous helium is determined readily from the perfect-gas law $\rho_{He} = P/RT$. Table 1 summarizes calculations of ρ_{He} and ρ_C. It is obvious from Eqs. (5) and (6) that $\mu_{He} \simeq \mu_s$ when $C \leq 0.5$. The curves for heat-transfer coefficients h in the upper part of Fig. 2 were calculated using Eq. (4) and values of $\mu_s (= \mu_{He})$, k_s, and c_{ps}, taken from the lower part of Fig. 2.

A sample calculation is as follows: For $T = 19°$, $P = 2116$, and $C = 0.1$, and with $k_C = 105$, $c_{pC} = 0.0013$, $k_{He} = 0.09$, $c_{pHe} = 1.3$, $\rho_C = 135$, and $\mu_{He} = 1.7$ (using units in Nomenclature), find h for a flow rate of 25 lb/hr through a ½-in.-i.d. tube. From Eq. (1), $k_s = 10.6$ Btu/hr-°R-ft²/in; from Eq. (2), $c_{ps} = 1.17$ Btu/lb-°R; from the perfect-gas law, $\rho_{He} = 0.287$ lb/ft³; and from Eq. (7), $\rho_s = 0.319$ lb/ft³, since $C < 0.5$, $\epsilon \simeq 1.0$, and $\mu_s \simeq \mu_{He} = 1.7$ lb/ft-sec. Using these values in Eq. (4), $h = 3.66$ Btu/hr-°R-ft².

Table 1 Densities of helium and suspension for $\epsilon \simeq 1.0$

C	T, °R	ρ_{He}, lb/ft³	ρ_s, lb/ft³
0.001	19	0.287	0.287
	90	0.068	0.068
	180	0.030	0.030
0.01	19	0.287	0.290
	90	0.068	0.069
	180	0.030	0.031
0.1	19	0.287	0.319
	90	0.068	0.076
	180	0.030	0.034
0.5	19	0.287	0.574
	90	0.068	0.136
	180	0.030	0.091

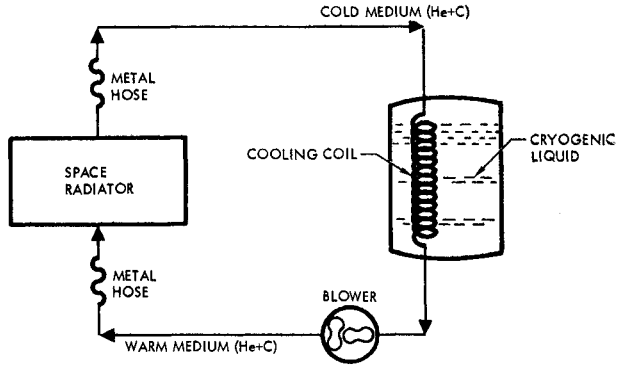

Fig. 1 Refrigeration by fluidized technique.

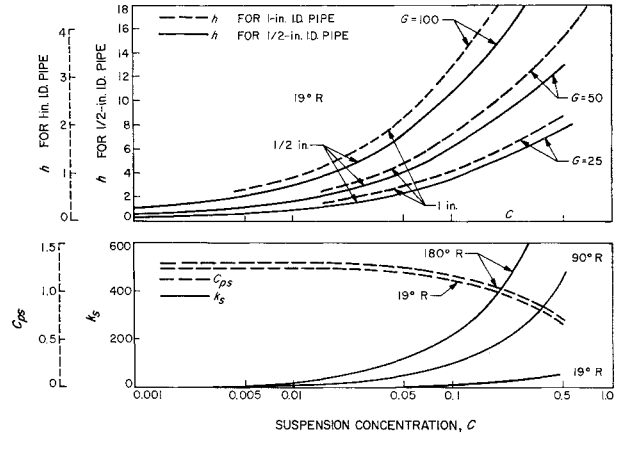

Fig. 2 Concentration of carbon suspension in helium vs k_s, c_{ps}, and h.

Conclusion

The success of the fluidized technique in refrigeration will depend, to a large extent, upon whether the suspended graphite particles can increase the thermal conductivity of the suspension and decrease the fluid film resistance on the walls of the heat exchanger as estimated herein. The estimated thermal conductivity increases rapidly with temperature ($T > 19°R$) and carbon concentration ($C > 0.01$). The estimated c_p decreases slightly as C is increased; it is insensitive to temperature. As a result, the convective heat-transfer coefficient for suspension can increase significantly by increasing the suspension operating temperature or concentration; for example, a tenfold increase in heat-transfer coefficient as compared to that of gaseous helium, can be obtained by adding 10% by weight of carbon dust. Suspensions containing other solid particles are under investigation. No attempt has been made yet to size the heat exchangers or radiators for any specific application.

References

[1] Hendel, F. J., "Gas liquefiers for space and lunar operations," 1962 Cryogenic Engineering Conference, Univ. of California, Los Angeles, Calif. (August 1962).

[2] Farbar, L. and Morley, M. J., "Heat transfer to flowing gas-solid mixtures in a circular tube," Ind. Eng. Chem. 49, 1143–1150 (1957).

[3] Zenz, A. F. and Othmer, D. F., *Fluidization and Fluid-particle Systems* (Reinhold Publishing Corp., New York, 1960).

Gyro Pendulum as a Vertical Reference for a Rotating Platform

E. E. Fisher*
Honeywell Inc., Minneapolis, Minn.

Introduction

It is known that a damped gyro pendulum with fixed point of support† will precess about the vertical and asymptotically reach a state of motion with its symmetry axis and angular momentum vector near vertical, thus acting as a vertical sensor. Motion of a gyro pendulum suspended on rotating platform is investigated here to determine its applicability as a vertical sensor.‡ In general, the platform's axis of rotation will not be along the vertical. A requirement is to determine the misalignment of the platform rotation axis from the vertical by observing the gyro pendulum-platform relative motion.

In a common gyro pendulum, alignment of its symmetry axis to the vertical is caused by viscous resistance to motions of this axis transversing the vertical. Thus, in steady state, such resistance vanishes. With the gyro pendulum suspended at a point on a rotating platform, the analogous resistance is platform-oriented and will not vanish with the symmetry axis aligned to vertical, should this occur. This effect, the Coriolis or gyroscopic forces, and the less interesting centrifugal forces are investigated below. It is shown that the resulting steady-state relative motion will be a coning of the symmetry axis about a line slightly displaced from the vertical at the platform's frequency of rotation. The offset is a result of the centrifugal forces. The motion will lag the motion of vertical with respect to the platform and will be directly proportional to the misalignment of the platform rotation axis from the vertical.

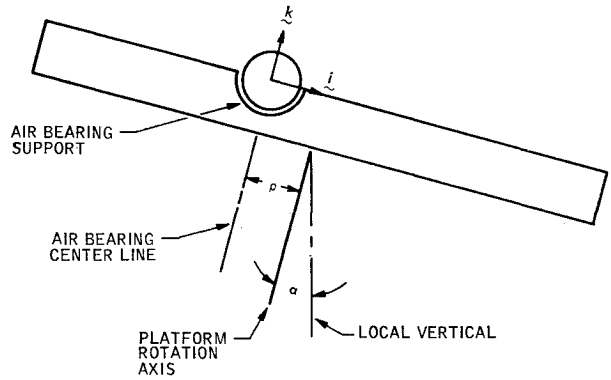

Fig. 1 Geometry at time $t = 0$.

Analysis

Consider a rotating platform with its axis of rotation tilted by a small angle α from the vertical, with an attached air bearing supporting a spherical pendulated rotor at a distance ρ from the axis of rotation (Fig. 1). The platform's centerline is assumed to be parallel to the centerline of the air bearing. A coordinate system **i**, **j**, **k** is fixed to the platform with its origin at the center of symmetry of the air bearing assumed to be the rotor's point of suspension.

The **k** axis is along the platform's axis of rotation. The **i** axis is orthogonal to **k** and in the plane determined by vertical and the platform rotation axis of time $t = 0$. It is assumed that total torque on the rotor about the **k** axis is zero; this is accomplished by spin jets symmetric with respect to this axis. A coordinate system **i′**, **j′**, **k′** is defined so that **k′** is along the rotor symmetry axis and **i′** and **j′** are in the equatorial plane of the rotor, not rotating about **k′** with the rotor (Fig. 2). θ and ϕ are small angles, as indicated. It is assumed that the transverse viscous torques are of the form $-k\dot{\theta}\mathbf{i}' - k\dot{\phi}\,\mathbf{j}'$, where k is an empirical drag coefficient. Such torques are introduced by using a drag pin and viscous dash-pot at the bottom of the rotor. If A is the transverse moment of inertia of the rotor, C is the moment of inertia about the **k′** axis, M is the rotor mass, g is the acceleration of

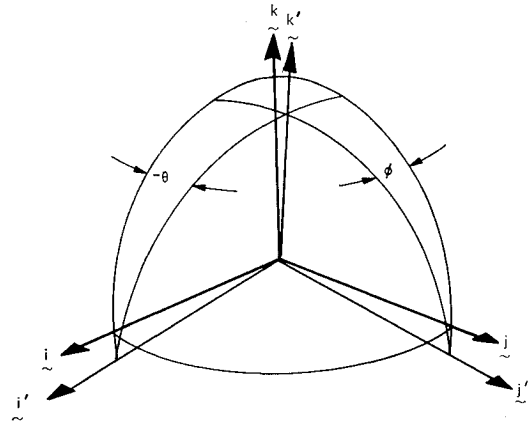

Fig. 2 Coordinate geometry.

Received September 30, 1964; revision received March 17, 1965. The author wishes to acknowledge Fulton Koehler of the University of Minnesota whose elegant lectures in the theory of the gyroscope have served to stimulate the author's interest in this phenomenon.

* Senior Research Scientist, Research Department, Systems and Research Division.

† A gyro pendulum is a symmetrical top with an earth-fixed point of suspension located on its axis of symmetry above the mass center.

‡ In this problem the point of suspension is again fixed in the top on its axis of symmetry above the mass center. However, since the point of suspension is also fixed to the rotating platform, it now rotates with respect to the earth at the platform rotation frequency.